

Adhesion of spheres by thin liquid films

By M. J. MATTHEWSON

IBM Almaden Research Center, 650 Harry Road,
San Jose, California 95120-6099, U.S.A.

[Received 24 July 1987 and accepted 7 September 1987]

ABSTRACT

Thin liquid films may produce significant adhesion between solid bodies, such as powder agglomerates and ultra-flat surfaces. The adhesive force can be split into two components; the meniscus force and a viscous component which, at sufficiently high deformation rates, will become dominant. This paper presents an analysis for the viscous component of adhesion acting between spheres coated by thin liquid layers, which is expressed as the impulse required to separate the spheres. This impulse depends on the radii and surface roughness of the spheres, and the fluid viscosity and thickness. The dependence on the roughness and quantity of fluid is unexpectedly weak (i.e. logarithmic). The predictions of the analysis are confirmed by direct experiment using a simple force pendulum.

§1. INTRODUCTION

The presence of a thin liquid film can significantly increase the adhesion between solid bodies. This phenomenon is particularly important to the strength of soils and agglomerates, powder transport properties, the adhesion of powders to surfaces and the adhesion between ultra-flat surfaces. The adhesive force can be divided into two components; a meniscus force and a rate-dependent viscous term. McFarlane and Tabor (1950) considered the meniscus force and showed that the force between a sphere and a flat surface is given by

$$F_m = 4\pi R\gamma \cos \alpha, \quad (1)$$

where R is the sphere radius, γ the liquid surface tension and α the contact angle. This equation applies strictly for film thicknesses very much smaller than R but a general treatment is given by Orr, Scriven and Rivas (1975). McFarlane and Tabor confirmed eqn. (1) by experiment using an elegantly simple force-pendulum apparatus. More recently Fisher and Israelachvili (1981) showed that eqn. (1) held for water meniscus radii down to 5 nm. However, McFarlane and Tabor observed that the full meniscus force was only realized provided the film thickness exceeded the combined roughnesses of the contacting surfaces. While the adhesive force is greatly reduced for very thin films or very rough surfaces, eqn. (1) can still be expected to describe the adhesive forces at individual asperity contacts.

McFarlane and Tabor observed experimentally that the viscous component of the adhesive force was significant for more viscous liquids (viscosity ~ 1 Pa s). By dimensional arguments they showed that the viscous term was given by

$$F_v = \beta\eta/t_s \quad (2)$$

where η is the viscosity and t_s is the time to separate the two surfaces. While experiment confirmed this relationship, the nature of the proportionality constant, β (dimension $[L]^2$), was not determined.

The viscous term is very important for highly viscous liquids, but also it can dominate for liquids of modest viscosity at high shear rates. An understanding of it is important therefore when considering the high-strain-rate properties of soils and agglomerates and the adhesion between ultra-flat surfaces when the asperity contact points are surrounded by liquid. In the latter case the extreme thinness of the liquid layer leads to very high shear rates within the liquid for small displacement rates of the surfaces. This paper derives an expression for the parameter β in eqn. (2) which is found to be in good agreement with experimental results for a wide range of sphere radius, liquid film thickness and surface roughness.

2. EXPERIMENTAL

The force pendulum technique of McFarlane and Tabor (1950) has been used to determine the adhesive force between a sphere and a flat, although a degree of automation has been added as shown in fig. 1. A sphere is suspended by a fine wire from a rigid support. A vertical flat plate upon which a thin liquid layer is spread, is moved by a computer-controlled motorized stage until it makes contact with the sphere. After a certain dwell time the plate is moved away taking the sphere with it. At some position the sphere pulls away from the flat and collides with the switch. The computer monitors the switch and is therefore able to record both the time and stage position at which the sphere detaches. The force applied to the sphere is given by

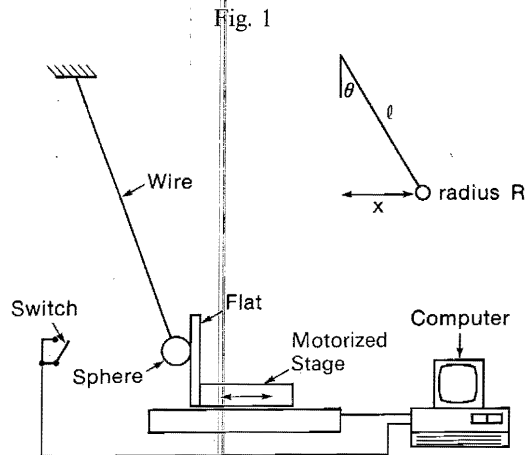
$$F = mg \tan \theta, \quad (3)$$

where m is the mass of the sphere and θ is the angle between the pendulum and the vertical. Except for the smallest spheres used, θ is small so that to a good approximation

$$F = mgx/l, \quad (4)$$

where l is the pendulum length and x the horizontal displacement of the sphere.

The motorized stage is of the d.c. servo type giving a smooth motion with speeds up to $400 \mu\text{m s}^{-1}$. While it can be programmed to give any velocity/time profile, only two types of experiment were performed for this work. Firstly, a 'static' experiment where



Schematic diagram of the force-pendulum apparatus.

the separation time is measured as a function of a constant applied force, and secondly a 'dynamic' experiment in which the adhesive force is measured as a function of the constant stage velocity, i.e. the applied force is ramped linearly with time.

A variety of materials were used for the sphere and flat but all gave results consistent with those presented here which are exclusively for sapphire spheres on glass plates. The radius of the liquid bridge between the sphere and the plate is measured by viewing through the plate. The sphere slides slowly across the surface of the plate during the dynamic experiments but this is observed to have a small effect on the shape of the bridge. The liquid used in these experiments, a branched 'Y' structured perfluoropolyether Fomblin lubricant, does not have a zero contact angle with either glass or sapphire but both surfaces are fully covered with the liquid so that the effective contact angle is zero, thus ensuring reproducible results. Equation (1) then reduces to

$$F_m = 4\pi R\gamma. \quad (5)$$

Some run-off of the liquid from the vertical plate does occur during the course of a series of experiments. To avoid systematic errors, readings under different conditions are interleaved so that each set of conditions experiences the same range of liquid film thickness.

The ambient temperature varies from 21.8 to 24.3°C between experiments. The values of the viscous component of adhesion are calculated for a 20°C environment by assuming an Arrhenius-type dependence of viscosity on temperature, given that, from tables, the viscosity falls from 2.9 Pa s at 20°C to 1.0 Pa s at 38°C. The correction factor, which depends only on the ratio of these two viscosities, varies by ~10% between experiments and its incorporation reduces the scatter in the results.

§3. ANALYSIS

It may be shown from dimensional arguments that at low Reynolds number the viscous force acting on a body moving through a fluid of viscosity η with a velocity $\dot{\xi}$ is

$$F_v = \eta L \dot{\xi}, \quad (6)$$

where L is a function of length parameters and has the dimension of length. Rearranging and integrating over a path producing complete separation gives

$$\int_0^\infty F_v dt = \eta \int_{\xi_0}^\infty L d\xi, \quad (7)$$

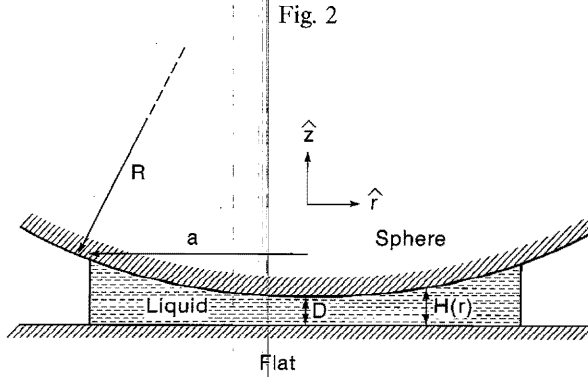
where ξ_0 is the starting value of the separation coordinate ξ . Since η is a constant and $\int_{\xi_0}^\infty L d\xi$ is a constant for a given path, $\int_0^\infty F_v dt$ must be a constant independent of the rate of motion along that path. Therefore the criterion for overcoming the viscous component of adhesion is conveniently expressed as a criterion on the viscous *impulse*

$$I_v = \eta \int_{\xi_0}^\infty L d\xi. \quad (8)$$

An expression for I_v appropriate to our experiments will now be determined.

Chan and Horn (1985) consider Reynolds' lubrication equation for the case of a sphere of radius R moving normal to a flat surface at a separation D and show that the pressure distribution, $P(r)$, over the spherical surface satisfies the equation

$$\frac{1}{r} \frac{d}{dr} \left[r H^3(r) \frac{dP(r)}{dr} \right] = 12\eta \dot{D}, \quad (9)$$



Geometry of the liquid bridge between a sphere and a flat surface.

where $H(r)$, the separation of the surfaces at a radius r (fig. 2) is

$$H(r) = D + (r^2/2R), \quad (10)$$

assuming $r \ll R$. Integrating (9) and applying the boundary condition that dP/dr is finite at $r=0$ gives

$$\frac{dP}{dr} = 6\eta D \frac{r}{H^3(r)}. \quad (11)$$

Chan and Horn integrate (11) with the boundary condition that $P(\infty)$ is the ambient pressure, and integrate this pressure over the sphere's surface to derive the viscous force

$$F_v = 6\pi\eta R^2 \dot{D}/D. \quad (12)$$

Their experimental results are in good agreement with eqn. (12) for D greater than the molecular dimensions of the fluid. However, this expression is unsuitable for the present work since it applies to the situation when the wetted region is of effectively infinite extent. The integration of eqn. (12) to calculate the impulse I_v required to separate the surfaces to infinity is divergent because of this. This analysis is now modified to be applicable when the wetted region is finite. If the wetted radius a is assumed to be in the range $R \gg a \gg D$ then edge effects may be ignored; namely, the liquid bridge may be taken as right-sided as in fig. 2, and the curvature of the meniscus may be ignored for all purposes except calculating the meniscus pressure. Equation (9) is integrated using the boundary condition $P(a) = B$, the ambient pressure, giving

$$P(r) = B + 3\eta R \dot{D} \left[\frac{1}{H^2(a)} - \frac{1}{H^2(r)} \right]. \quad (13)$$

The total force acting on the sphere in the \hat{z} direction (assuming that the curved surface is approximately perpendicular to the \hat{z} direction since $R \gg a$) is given by

$$F_v = \int_0^a 2\pi r [B - P(r)] dr = 6\pi\eta R^2 \left[1 - \frac{D}{H(a)} \right]^2 \frac{\dot{D}}{D}, \quad (14)$$

which reduces to (12) for large $H(a)$. The volume of the liquid bridge

$$V = \int_0^a 2\pi r H(r) dr = \pi R [H^2(a) - D^2] \quad (15)$$

is assumed to be conserved as the sphere is removed from an initial separation from the surface of D_0 and wetted radius a_0 so that eqn. (15) describes the changing shape of the bridge. The viscous impulse is defined by

$$I_v = \int_{D_0}^{\infty} 6\pi\eta R^2 \left[1 - \frac{D}{H(a)} \right]^2 \frac{dD}{D}, \quad (16)$$

which becomes, using the relationship between $H(a)$ and D in eqn. (15),

$$I_v = 6\pi\eta R^2 \ln \left[\frac{(D_0 + H(a_0))^2}{4D_0 H(a_0)} \right]. \quad (17)$$

For $H(a_0) \gg D_0$ (which is the case for the experiments described here) this simplifies to

$$I_v = 6\pi\eta R^2 \ln(a_0^2/8RD_0). \quad (18)$$

If it is assumed that the liquid in the bridge is derived from a film of thickness t and that no extra liquid is 'wicked' in from the surrounding film, then provided $t \gg D_0$ we have

$$V = \pi a_0^2 t, \quad (19)$$

so that from (18)

$$I_v = 6\pi\eta R^2 \ln(t/2D_0) \quad (20)$$

giving the perhaps surprising result that the viscous adhesion is a relatively weak function of the film thickness and the distance of closest approach (a characteristic of the surface roughness). For the case of two spheres of radii R_1 and R_2 , the value of R in the above equations is replaced by the effective radius found by summing the surface curvatures, $(1/R) = (1/R_1) + (1/R_2)$. It will now be shown how I_v is determined in the static and dynamic pendulum experiments.

3.1. 'Static' adhesion

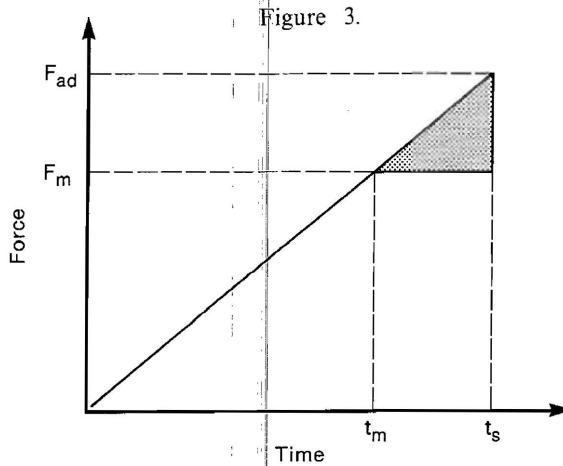
For a constant force, eqn. (7) and (8) reduce to

$$I_v = F_v t_s, \quad (21)$$

where t_s is the separation time. Assuming that the meniscus force does not vary during separation the adhesive force is given by

$$F_{ad} = F_m + F_v = F_m + (I_v/t_s) \quad (22)$$

so that a plot of $(1/t_s)$ against F_{ad} yields a straight line of slope $(1/I_v)$ and intercept with the force axis F_m .



Force/time relationship for the 'dynamic' experiment showing the viscous contribution (shaded area).

3.2. 'Dynamic' adhesion

Figure 3 shows schematically how the applied force varies with time for the dynamic experiment. For an applied force less than the meniscus force there is no tendency for the surfaces to separate. When the force exceeds F_m (at time t_m) then the viscous component is the excess over F_m . If F_m is constant then the total viscous impulse is given by the shaded area so that

$$I_v = \frac{1}{2}(F_{ad} - F_m)(t_s - t_m), \quad (23)$$

but since $F = \dot{F}t$ and $\dot{F} = mgv/l$ from eqn. (4) (v is the velocity of the plate \dot{x}) the adhesion is given by

$$F_{ad} = F_m + \left(\frac{2mgI_v}{l}\right)^{1/2} \sqrt{v}, \quad (24)$$

predicting a linear relationship between adhesion and square-root velocity whose slope determines I_v .

3.3. Variation of meniscus force

In the preceding analysis it is assumed that the meniscus force F_m is a constant. However, as the two surfaces separate, F_m reduces and it is readily shown that

$$F_m = 4\pi\gamma R[1 - D/H(a)]. \quad (25)$$

The equation of motion for the sphere, ignoring inertial terms, is

$$F = 4\pi\gamma R \left(1 - \frac{D}{H(a)}\right) + 6\pi\eta R^2 \left(1 - \frac{D}{H(a)}\right)^2 \frac{\dot{D}}{D}, \quad (26)$$

where F , the applied force, is a constant in the static experiment and $\dot{F}t$ in the dynamic case. The correction term to eqn. (5) in eqn. (25) has a small effect since the meniscus force decays more slowly with increasing D than the viscous force. However, eqn. (26) has been solved numerically and will be compared with the linearized relationships of eqns. (22) and (24).

3.4. Distance of closest approach

It is necessary to interpret the meaning of the distance of closest approach D_0 . Greenwood and Tripp (1967) consider the contact between a sphere and a rough surface and define the dimensionless load

$$T = (2P/\sigma E')(2R\sigma)^{1/2}$$

where P is the load, E' is an effective combined modulus for the two materials and σ is a measure of the surface roughness. For the experiments described here T is always less than $\sim 10^{-1}$ so that the work of Greenwood and Tripp (1967) indicates a low-load regime which is non-Hertzian; that is, that the sphere is supported by a few high asperities and does not make intimate contact with the flat surface. The distance of closest approach D_0 may then be interpreted as a measure of the local roughness at the contact zone. The table shows values of D_0 estimated by careful examination of profiles of the surfaces of the sapphire spheres and the three types of glass surface used (as-received, abraded and bead-blasted). The values of D_0 are not closely linked to the r.m.s. surface roughness since, particularly for the abraded and blasted surfaces, the sphere/flat contact zone is smaller than larger scale surface irregularities. D_0 is therefore estimated by eye from the profiles and the uncertainty in the estimates is reflected in an assumed 25% confidence interval. For contact on the as-received glass surface the spheres' roughness dominates, while the glass roughness dominates for the other two types of glass surface.

Values of D_0 estimated for the various surfaces.

Surface	D_0
Sapphire sphere	20 nm
As-received glass	2 nm
Abraded glass	100 nm
Bead-blasted glass	5 μm

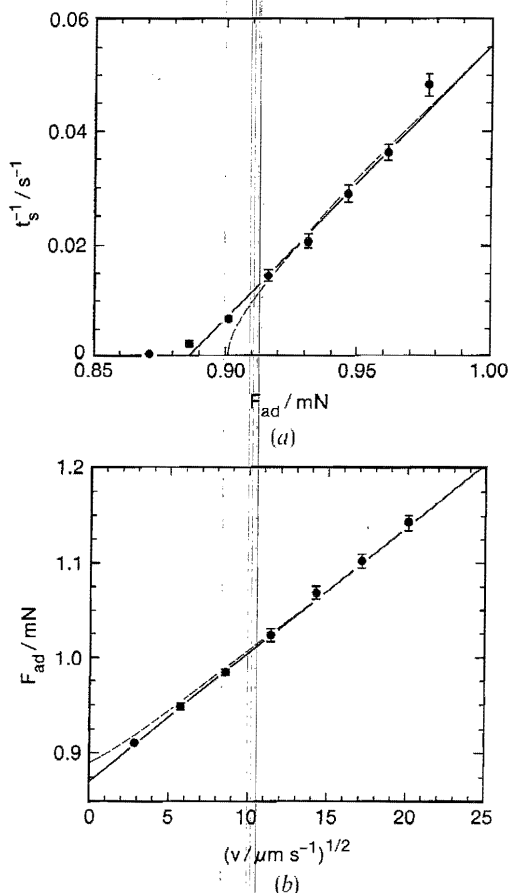
The adhesive force was found to be independent of the dwell time of the sphere on the glass surface for times in the range 1 and 1000 s. It may therefore be assumed that an equilibrium value of D_0 is reached prior to the start of each experiment for the standard 60 s dwell time used.

§ 4. EXPERIMENTAL RESULTS

Figure 4(a) shows typical results for a static experiment using a 4 mm radius ball on the as-received glass surface. Each point represents the average of ten measurements; error bars represent \pm one standard error in the mean. Except for very long and very short separation times, the data lie on a well defined straight line giving values of $F_m = 0.886 \pm 0.01$ mN and $I_v = 2.06 \pm 0.04$ mN s. The dashed line shows the numerical solution of eqn. (26) using $F_m = 0.901$ mN and $I_v = 2.46$ mN s. Agreement between the two lines is reasonable though somewhat different values of F_m and I_v are obtained.

The deviation of the data from linearity at short separation times is readily explained since the time taken for the motor drive to apply the force at its top velocity is comparable with the separation time. The deviation from linearity at long separation times is more interesting since the applied force is then less than the extrapolated meniscus force, yet at 0.87 mN the sphere separates in all experiments though the separation time is long (hours) and highly variable. This effect is thought to be due to

Fig. 4

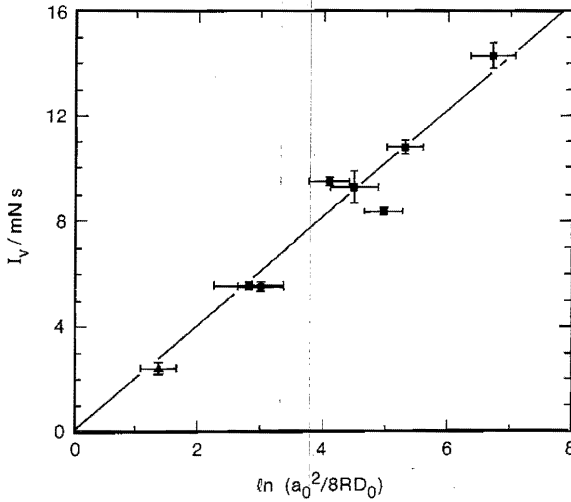


Results of (a) 'static' and (b) 'dynamic' adhesion measurements for the 4 mm-radius sapphire sphere on abraded glass.

vibrations, from which the apparatus is not fully isolated, setting up a squeeze bearing which gives an effective repulsion between the surfaces. This effect is small since the minimum adhesion force is lowered by only a few per cent.

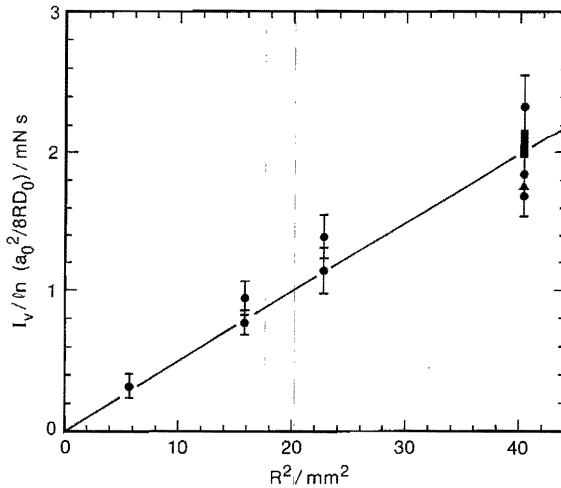
The dynamic experiment is found to be very much more convenient than the static experiment because it is not necessary to determine in advance the experimental window defined on one hand by the meniscus force and on the other by the motor's top speed. Figure 4(b) shows results for the dynamic experiment performed at the same time and under the same conditions as the static experiment of fig. 4(a) by interleaving measurements. The data lie close to a straight line verifying the form of eqn. (24) and linear regression gives values of $F_m = 0.871 \pm 0.001$ mN and $I_v = 3.00 \pm 0.08$ mN s, in reasonable agreement with the static experiment. The dashed line is a rough fit of a numerical solution of eqn. (26) using $F_m = 0.901$ mN and $I_v = 3.004$ mN s. Clearly, apart from a small systematic underestimate of the meniscus force, there is excellent agreement between linear regression and the more sophisticated function. In subsequent experiments I_v is measured by performing linear regression on data from dynamic experiments.

Fig. 5



Viscous impulse as a function of $\ln [a_0/(2RD_0)]$ for the 6.35 mm ball on as-received (■), abraded (●) and bead-blasted (▲) glass surfaces.

Fig. 6

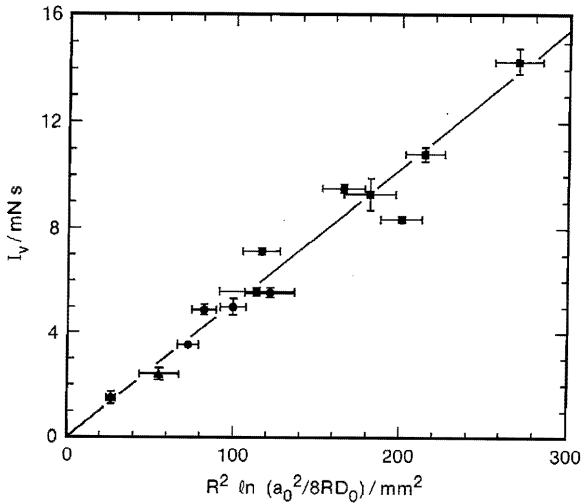


Viscous impulse as a function of sphere radius for contact on the abraded glass surface. Key as for fig. 5.

Figure 5 shows the variation of the viscous impulse I_v with the logarithmic component of the expression for I_v in eqn. (18) for a 6.35 mm sphere contacting the three different types of glass surface. A linear relationship is confirmed. These data span almost four decades in roughness (i.e. D_0) and one in a_0 (equivalent to two decades in film thickness, eqn. (20)) but I_v only varies by a factor of six.

Figure 6 shows the variation of I_v with R^2 for contact with the abraded glass surface. Here I_v is normalized to the logarithmic factor in eqn. (18) to remove the effect of some

Fig. 7



Combined data of figs. 5 and 6. Key as for fig. 5.

variability in the film thicknesses. Again the anticipated linear relationship is observed. Figure 7 combines the data of figs. (5) and (6). The slope of the regression line ($6\pi\eta$) gives a value of $\eta = 2.73 \pm 0.02$ Pa s which compares well with the value of 2.87 Pa s obtained from tables (internal communication).

Measurements of the meniscus force are in close agreement with eqn. (5). γ is measured to be 18 ± 1 mN m⁻¹ at the ambient temperature of $\sim 22^\circ\text{C}$ compared with the tabulated value of 21 mN m⁻¹ at 20°C .

§ 5. DISCUSSION AND CONCLUSIONS

An equation has been derived for the viscous component of adhesion between spheres due to a thin liquid film. The viscous term is represented by an impulse required to separate the two surfaces. The expression for this impulse has been confirmed by direct experiment using a simple force pendulum. The impulse is sensitive to the sphere radius (proportional to the square) but has only a weak logarithmic dependence on the film thickness and surface roughnesses. These results are particularly significant to the strength properties of powder materials and the adhesion of ultra-flat surfaces in the presence of small quantities of liquid.

The force-pendulum technique has been extended to a dynamic experiment in which the applied force increases linearly in time. This method is more convenient and provides more accurate results than the static experiment at constant applied force. A simple approximate solution for the motion of the surfaces during separation compares closely with a more exact numerical solution. Thus, the viscous and meniscus components to adhesion can be separated by straightforward linear regression to experimental data.

REFERENCES

- CHAN, D. Y. C., and HORN, R. G., 1985, *J. chem. Phys.*, **83**, 5311.
 FISHER, L. R., and ISRAELACHVILI, J. N., 1981, *J. Colloid Interface Sci.*, **80**, 528.
 GREENWOOD, J. A., and TRIPP, J. H., 1967, *J. appl. Mech.*, **34**, 153.
 MCFARLANE, J. S., and TABOR, D., 1950, *Proc. R. Soc., Lond. A*, **202**, 224.
 ORR, E. M., SCRIVEN, L. E., and RIVAS, A. P., 1975, *J. Fluid Mech.*, **67**, 723.